

Dynamic balance and gait impairments in Parkinson's disease: novel cholinergic patterns

Nicolaas I. Bohnen¹⁻⁵, Uros Marusic^{6,7}, Stiven Roytman¹, Rebecca Paalanen², Fotini Michalakis^{1,3},
Taylor Brown^{1,3,5}, Peter J.H. Scott¹, Giulia Carli^{2,3}, Roger L. Albin,²⁻⁵ & Prabesh Kanel^{1,3-4}

¹ Department of Radiology, University of Michigan, Ann Arbor, MI, USA

² Department of Neurology, University of Michigan, Ann Arbor, MI, USA

³ Morris K. Udall Center of Excellence for Parkinson's Disease Research, University of Michigan, Ann Arbor, MI, USA

⁴ Parkinson's Foundation Research Center of Excellence, University of Michigan, Ann Arbor, MI, USA

⁵ Neurology Service and GRECC, VA Ann Arbor Healthcare System, Ann Arbor, MI, USA

⁶ Institute for Kinesiology Research, Science and Research Centre Koper, Koper, Slovenia, EU

⁷ Department of Health Sciences, Alma Mater Europaea – ECM, Maribor, Slovenia, EU

* Correspondence:

Nicolaas I. Bohnen, MD, PhD, Functional Neuroimaging, Cognitive and Mobility Laboratory,
Departments of Radiology and Neurology, University of Michigan, 24 Frank Lloyd Wright Drive, Box
362, Ann Arbor, MI 48105-9755, USA. TEL: 734 936 5388; FAX: 734 998 8403. E-mail:

nbohnen@umich.edu

Short title: "Gait and Balance in PD: Cholinergic Patterns"

Abstract

The cholinergic system has been implicated in postural deficits, in particular falls, in Parkinson's disease. Falls and freezing of gait typically occur during dynamic and challenging balance and gait conditions, such as when initiating gait, experiencing postural perturbations, or making turns. However, the precise cholinergic neural substrate underlying dynamic postural and gait changes remains poorly understood. The aim of this study was to investigate whether brain vesicular acetylcholine transporter binding, as measured with [^{18}F]-fluoroethoxybenzovesamicolbinding PET, correlates with dynamic gait and balance impairments in 125 patients with Parkinson's disease (mean age 66.89 ± 7.71 years) using the abbreviated Balance Evaluation Systems Test total and its four functional domain sub-scores (anticipatory postural control, reactive postural control, dynamic gait, and sensory integration). Whole brain false discovery-corrected ($P < 0.05$) correlations for total abbreviated Balance Evaluation Systems Test scores included the following bilateral or asymmetric hemispheric regions: gyrus rectus, orbitofrontal cortex, anterior part of the dorsomedial prefrontal cortex, dorsolateral prefrontal cortex, cingulum, frontotemporal opercula, insula, fimbria, right temporal pole, mesiotemporal, parietal and visual cortices, caudate nucleus, lateral and medial geniculate bodies, thalamus, lingual gyrus, cerebellar hemisphere lobule VI, left cerebellar crus I, superior cerebellar peduncles, flocculus, and nodulus. No significant correlations were found for the putamen or anteroventral putamen. The four domain-specific sub-scores demonstrated overlapping cholinergic topography in the metathalamus, fimbria, thalamus proper, and prefrontal cortices but also showed distinct topographic variations. For example, reactive postural control functions involved the right flocculus but not the upper brainstem regions. The anterior cingulum associated with reactive postural control whereas the posterior cingulum correlated with anticipatory control. The spatial extent of associated cholinergic system changes were least for dynamic gait and sensory orientation functional domains compared to the anticipatory and reactive postural control functions. We conclude that specific aspects of dynamic balance and gait deficits in Parkinson's disease associate with overlapping but also distinct patterns of cerebral cholinergic system changes in numerous brain regions. Our study also presents novel evidence of cholinergic topography involved in dynamic balance and gait in Parkinson's disease that have not been typically associated with mobility disturbances, such as the right anterior temporal pole, right anterior part of the dorsomedial prefrontal cortex, gyrus rectus, fimbria, lingual gyrus, flocculus, nodulus and right cerebellar hemisphere lobules VI and left crus I.

Keywords: Parkinson's disease; dynamic balance; cholinergic; PET

Introduction

Gait impairments, balance issues, and falls stand as significant hallmarks of Parkinson's disease (PD), markedly reducing quality of life, escalating healthcare expenses, and amplifying the burden on caregivers.^{1,2} As the condition progresses, debilitating postural instability and gait difficulties become increasingly prevalent.³ These motor impairments pose considerable therapeutic challenges, typically showing increasing refractoriness to dopaminergic treatments.⁴⁻⁶ This indicates that other neurotransmitter systems may also play a pivotal role in regulating gait and balance changes in PD besides the dopaminergic system. In line with this understanding, our previous imaging studies revealed alterations in the cholinergic system associated with both freezing of gait and falls in PD.^{7,8} Specifically, falls were associated with cholinergic deficits in the thalamus, primarily the right lateral geniculate nucleus, whereas freezing of gait was associated with reduced vesicular acetylcholine transporter binding in striatal cholinergic interneurons and the limbic archicortex.⁸ Our recent work also demonstrated that loss of cholinergic nerve terminals in the medial geniculate nucleus, an important multisensory (particularly auditory and vestibular) processing metathalamic relay station, associates robustly with ratings of non-episodic balance impairments.⁹ In our previous acetylcholinesterase PET studies, we established a correlation between the pedunclopontine nucleus-thalamic binding of [¹¹C]-methylpiperidin-4-yl propionate ([¹¹C]-PMP) and postural sensory integration, an important function of postural control.¹⁰ We also demonstrated that the right hemispheric vestibular cortical cholinergic system plays a role in maintaining balance, especially during visual-vestibular integration tasks.¹¹ However, both studies had limitations due to the constraints of the [¹¹C]-PMP radioligand, precluding the examination of high-binding brain areas, such as the striatum and cerebellum. The introduction of vesicular acetylcholine transporter [¹⁸F]-fluoroethoxybenzovesamicol ([¹⁸F]-FEOBV) PET has opened new avenues for in vivo quantification of the presynaptic cholinergic system. This radiotracer provides highly detailed and specific imaging of cholinergic neurons, enabling precise estimation of ligand binding in regions densely populated with cholinergic terminals, such as the subcortical gray matter regions.¹²

Episodic mobility disturbances, such as falls and freezing of gait, typically occur during dynamic and challenging balance and gait conditions, such as when initiating gait, experiencing postural perturbations, making turns, walking in dim light, or on uneven surface. However, the precise cholinergic neural substrate underlying dynamic postural and gait remains poorly understood. Therefore, the main purpose of the present study was to explore whether regional cerebral [¹⁸F]-FEOBV binding associates with specific impairments of gait and balance, as assessed by the abbreviated Balance Evaluation Systems Test (Mini-BESTest), in patients with PD. The Mini-BESTest incorporates four sub-categories of dynamic

1
2 balance and gait conditions: anticipatory postural control, reactive postural control, dynamic gait, and
3 sensory orientation. Previous research has demonstrated the high interrater reliability, construct validity,
4 and test/retest reliability of the MiniBESTest within a PD cohort.^{13–15} The MiniBESTest has also been
5 found to independently predict falls and provides a robust measurement of dynamic balance and gait in
6 PD populations.^{16,17} For this study, we performed whole-brain voxel-based [¹⁸F]-FEOBV PET correlation
7 analysis with the total summed score as primary analysis and the four functional domain sub-conditions
8 as post-hoc exploratory analyses. Our overall hypothesis was that cholinergic system changes underlying
9 greater difficulty on dynamic balance and gait conditions involve more widespread supra- and
10 infratentorial brain regions that may partially overlap but also may be topographically distinct among the
11 four functional MiniBESTest conditions.
12
13
14
15
16
17
18
19

20 **Materials and methods**

21 **Subjects**

22
23
24
25
26
27 A sample of 125 predominantly male (males=97, females=28) PD patients participated in the present
28 cross-sectional study. On average, the participants were 66.89±7.71 years old, and have had motor
29 symptoms for 6.12±4.77 years. All participants in the present study satisfied the UK Parkinson's Disease
30 Society Brain Bank criteria for clinical diagnosis of Parkinson's disease.¹⁸ Based on Hoehn & Yahr (HY)
31 staging, most participants in this study had moderate disease severity (HY₂₋₃=108), and relatively few
32 participants presented with mild (HY_{<2}=12) or severe disease (HY_{>3}=5). Group averaged HY stage was
33 2.43±0.60. Sixty-seven participants were treated with carbidopa-levodopa alone, 38 were on a combined
34 regiment of carbidopa-levodopa and dopamine agonists, 9 participants were only taking dopamine
35 agonists with no carbidopa-levodopa, and the remaining 11 participants were receiving neither carbidopa-
36 levodopa nor dopamine receptor agonists. None of the participants in the present study were prescribed
37 anti-cholinergic or cholinesterase inhibitor drugs. Anatomical imaging evidence of major intracranial
38 lesion including large vessel strokes were exclusionary to participation in the study. Correlational findings
39 pertaining to total axial motor deficit ratings and regional cholinergic nerve terminal integrity were
40 obtained from an overlapping participant cohort and published on previously.⁹
41
42
43
44
45
46
47
48
49
50
51

52 **Clinical assessments**

53
54
55 The Movement Disorder Society-revised Unified Parkinson's Disease Rating Scale motor examination
56 was administered to study participants in the morning, before they took their regularly prescribed
57
58
59
60

dopaminergic medications ('off' state).¹⁹ The mean motor examination score on the Movement Disorder Society-revised Unified Parkinson's Disease Rating Scale part three was 35.69 ± 13.31 (range 9-76). Subjects completed the Montreal Cognitive Assessment.²⁰ Mean Montreal Cognitive Assessment scores were 26.26 ± 2.83 . The levodopa equivalent dose was computed as described previously.²¹

Abbreviated balance evaluation systems test (Mini-BESTest)

The Mini-BESTest assesses dynamic balance and gait functions and includes fourteen items scored from zero to two, providing sub-scores for anticipatory postural control, reactive postural control, dynamic gait, and sensory orientation.²² The Mini-BESTest has a minimum score of zero and a maximum score of twenty-eight, with a lower score reflecting balance and gait difficulties. The Mini-BESTest was performed in the dopaminergic medication 'off' state. See **Figure 1**.

Imaging and statistical analysis

Study participants underwent a brain MRI scan in a 3 Tesla Philips Achieva system (Philips, Best, The Netherlands). Biograph 6 TruPoint PET/CT scanner (Siemens Molecular Imaging, Inc., Knoxville, TN) in 3D imaging mode was used to administer the PET imaging protocol.⁹ [¹⁸F]-FEOBV preparation was done as previously described.²³ Six delayed dynamic imaging frames (5-minute frames, 30 minutes total) were acquired 3 hours after an intravenous bolus dose injection of 8 mCi [¹⁸F]-FEOBV.²⁴ Scatter and motion artifact correction was applied to the resulting dynamic PET images.⁹ Distribution volume ratio (DVR) parametric [¹⁸F]-FEOBV PET images were obtained using a non-invasive supratentorial white matter reference tissue approach.^{25,26} DVRs were calculated by summing the dynamic imaging frames across time and dividing the resulting summed image by the mean of the voxelwise signal observed in the reference tissue.²⁶ Statistical parametric mapping (SPM) software (SPM12; Wellcome Trust Centre for Neuroimaging, University College, London, England [<https://www.fil.ion.ucl.ac.uk/spm/software/spm12/>]) was used to perform MRI-PET registration and partial volume correction on the resulting parametric PET images.⁹

1 Whole-brain voxel-based [^{18}F]-FEOBV PET and Mini-BESTest total score and sub-scores
2 correlational analyses were performed using parametric SPM12 or non-parametric (SnPM) software after
3 adjustment for levodopa equivalent dose dependent on the data distribution. Cluster peak analyses were
4 also performed on clusters with a minimum of 50 voxels with location of the peak voxel in Montreal
5 Neurological Institute (MNI X-Y-Z space), peak voxel (pseudo) t-score, applicable Brodmann areas (BA),
6 and the associated network regions reported for each valid cluster. For both the whole brain voxel-based
7 and the peak cluster analysis significance thresholds after false discovery (FDR) correction were set at P
8 < 0.05 . Trending correlations which fail to survive FDR correction are presented at uncorrected threshold
9 of $P < 0.001$.

10 To assess the extent of shared clinicometric variance between the MiniBEST subscores, a partial
11 correlation analysis was performed. For each MiniBEST subscore, a multiple linear regression model was
12 fitted predicting that subscore from all the other subscores. Proportion of variance in each MiniBEST
13 subscore shared with other subscores was evaluated using the coefficient of determination (R^2) of the
14 resulting model. Correlational structure of the MiniBEST subscores was examined by tabulating the
15 standardized regression coefficients (β) of the resulting multiple regression models as a partial correlation
16 matrix.

17 **Standard protocol approval, registration, and subjects' consent**

18 This study (ClinicalTrials.gov Identifiers: NCT02458430 & NCT01754168) was approved by the
19 Institutional Review Boards of the University of Michigan and the Ann Arbor Veterans Affairs Healthcare
20 System. All participants provided written informed consent.

21 **Results**

22 **MiniBEST subscore partial correlation analysis**

23 The tabulated partial correlation matrix along with model R^2 values corresponding to each of the
24 MiniBESTest subscores can be found in Table 1. About 30-50% of variance in each subscore appears
25 shared with the other subscores, meaning that at least about half of the variance in each subscore is unique
26 to that subscore. The partial correlation structure of MiniBESTest subscores suggests that the anticipatory
27 postural control subscore is most strongly related to the MiniBEST sensory subscore, but also
28 demonstrates significant association with all the other subscores. In contrast, the reactive postural control
29

1
2 subscore appears to significantly associate only with the anticipatory subscore. Dynamic gait subscore
3 associates most strongly with the sensory but also significantly with anticipatory subscore, while sensory
4 subscore associates with both dynamic gait and anticipatory subscore to an approximately equal extent.
5
6
7
8
9

10 **Whole brain vesicular acetylcholine transporter PET voxel-based** 11 **correlations with total Mini-BESTest scores** 12 13 14

15 The whole brain voxel-based correlation analysis (FDR-corrected, $P < 0.05$) unveiled significant
16 correlations between vesicular acetylcholine transporter binding and total Mini-BESTest scores across
17 distinct brain clusters. These correlations encompassed specific brain regions, including frontotemporal
18 areas such as the gyrus rectus, orbitofrontal regions, right anterior dorsomedial prefrontal cortex (upper
19 medial BA 10 and BA 9), bilateral dorsolateral prefrontal cortex, all segments of the cingulum, bilateral
20 insula, right more than left frontotemporal operculum, bilateral mesiotemporal cortex, left mid posterior
21 temporal cortex, right more than left fimbriae/isthmus cingulum, right temporal pole, left more than right
22 peri-central cortex. Subcortical areas involved bilateral caudate nuclei, metathalami (lateral and medial
23 geniculate bodies) and thalami proper. Additionally, correlations extended to the occipito-parietal cortices,
24 including the right parietal cortex, occipital cortex, right more than left lingual gyri. Furthermore,
25 distinctive correlations were evident in the cerebellum, particularly the right cerebellar hemisphere lobule
26 VI, left cerebellar crus I, bilateral superior cerebellar peduncles, nodulus, right flocculus, and upper dorsal
27 vermis. No significant correlations were present for the putamen and anteroventral striatum (nucleus
28 accumbens; Figure 2, Table 2). Peak cluster analysis findings (FDR significant $P < 0.05$) are shown in
29 Supplemental Table 1. Most extensive clusters were centered around the right hippocampus, right superior
30 frontal gyrus, right inferior frontal gyrus triangular part, and left more than right precentral cortices. The
31 same analysis was repeated with a stricter voxelwise statistical threshold (FDR-corrected, $P < 0.01$), see
32 supplementary figure 1.
33
34
35
36
37
38
39
40
41
42
43
44
45
46

47 **Whole brain vesicular acetylcholine transporter PET voxel-based** 48 **correlations with anticipatory postural control subscore** 49 50 51

52 Similar to the findings observed for the Mini-BESTest total score, the whole brain voxel-based correlation
53 analysis (FDR-corrected, $P < 0.05$) revealed a significant correlation between the anticipatory postural
54 control subtest and regional vesicular acetylcholine transporter binding. These correlations were identified
55
56
57
58
59
60

1
2 in brain clusters topographically situated across frontotemporal cortices, subcortical regions, occipito-
3 parietal cortices, and the cerebellum. While the frontotemporal correlation was less extensive compared
4 to the total score, it notably involved similar brain regions: bilateral gyrus rectus, bilateral orbitofrontal
5 regions, anterior cingulum, bilateral dorsolateral prefrontal cortex (BA 8 and 9), right more than left
6 frontotemporal operculum, right insula, bilateral fimbriae/isthmus cingulum, and right temporal pole. The
7 lower vesicular acetylcholine transporter binding observed in bilateral caudate nuclei, lateral and medial
8 geniculate bodies, and thalami proper exhibited a significant correlation with lower anticipatory postural
9 control subtest scores, aligning with the correlation found in the Mini-BESTest total score. Additionally,
10 significant correlations were identified between anticipatory postural control scores and vesicular
11 acetylcholine transporter binding in occipito-parietal cortices and cerebellar areas, consistent with the
12 findings outlined in the total Mini-BESTest scores section (Figure 3, Table 2). Notably, the right parietal
13 cortex and flocculus exhibited no significant correlation in this case. The anticipatory postural control
14 subset scores exhibited a positive correlation with the brainstem (mesencephalic tectum). There were no
15 significant correlations observed for the putamen and anteroventral striatum. Peak cluster analysis
16 findings (FDR significant $P < 0.05$) are shown in Supplemental Table 2. Most extensive clusters were
17 centered around the left thalamus, right insula, left medial superior frontal gyrus, and left precentral cortex
18 regions.
19
20
21
22
23
24
25
26
27
28
29
30

31 32 **Whole brain vesicular acetylcholine transporter PET voxel-based** 33 **correlations with reactive postural control subscore** 34 35 36 37

38 The whole brain voxel-based correlation analysis (FDR-corrected, $P < 0.05$) revealed extensive
39 correlations between reactive postural control subtest scores and regional vesicular acetylcholine
40 transporter binding within frontotemporal regions, including bilateral gyrus rectus, bilateral orbitofrontal
41 cortex, predominantly the right anterior parts of the dorsomedial prefrontal cortex (upper medial BA 10
42 and BA 9), bilateral dorsolateral prefrontal cortex (BA 8 and 9), anterior cingulum, left-dominant
43 frontotemporal operculum, bilateral insula, bilateral mesiotemporal lobes, bilateral fimbriae/isthmus
44 cingulum, left peri-central cortex, right temporal pole, inferior temporal lobes, and left mid and posterior
45 temporal lobe. Additionally, significant correlations emerged in subcortical structures, notably involving
46 bilateral caudate nuclei, lateral and medial geniculate nuclei, and the left pulvinar. Significant correlations
47 were observed also in parietal and cerebellar regions, albeit more limited compared to the Mini-BESTest
48 total and anticipatory postural control scores, encompassing the right parietal cortex, right flocculus,
49 nodulus, and bilateral superior cerebellar peduncles (Figure 4, Table 2). Notably absent were the putamen,
50
51
52
53
54
55
56
57
58
59
60

1 anteroventral striatum, right cerebellar lobule VI, brainstem, and visual cortex. Peak cluster analysis
2 findings (FDR significant $P < 0.05$) are shown in Supplemental Table 3. Most extensive clusters were
3 centered around the right superior frontal gyrus, left precentral, left postcentral, right inferior frontal gyrus
4 triangular part, and left inferior temporal gyrus regions.
5
6
7
8
9

10 **Whole brain VACHT PET voxel-based correlations with dynamic gait** 11 **subscore** 12 13

14 Whole brain voxel-based correlation analysis (non-corrected at $P = 0.001$) showed correlations between
15 the DG subtest scores and regional vesicular acetylcholine transporter binding in the following regions:
16 dorsolateral prefrontal cortex (BA 8 and 9), right insula, bilateral mesiotemporal, bilateral mid posterior
17 temporal cortex, right fimbriae/isthmus cingulum, right lateral geniculate nucleus, bilateral superior
18 thalami, brainstem (pedunculopontine nucleus - laterodorsal tegmentum (PPN/LTD) and tectum), and
19 right cerebellar hemisphere lobule VI (Figure 5, Table 2). Absent were the gyrus rectus, orbitofrontal
20 regions, cingulum, anteromesial frontal regions, right temporal pole, caudate nuclei, The extent of
21 involved topography was substantially less compared to the anticipatory postural control and reactive
22 postural control Mini-BESTest sub-score correlations. Peak cluster analysis findings (non-corrected at P
23 < 0.001) are shown in Supplemental Table 4. Most extensive clusters were centered around the bilateral
24 thalamic complexes, bilateral superior frontal gyri, right hippocampus and left para-hippocampal gyrus
25 regions.
26
27
28
29
30
31
32
33
34
35
36

37 **Whole brain vesicular acetylcholine transporter PET voxel-based** 38 **correlations with sensory orientation subscore** 39 40

41
42
43
44
45
46
47
48
49
50
51
52
53
54
55
56
57
58
59
60
Voxel-based correlation analysis (non-corrected at $P = 0.001$) showed correlations between the sensory
orientation subtest scores and regional vesicular acetylcholine transporter binding in the left anterior
dorsomedial prefrontal cortex (upper medial BA 10 and BA 9), right more than left dorsolateral prefrontal
cortex (BA 8 & 9), bilateral hippocampi, bilateral fimbriae/isthmus cingulum, left caudate nucleus, right
more than left lateral geniculate nuclei, left medial geniculate nucleus, left dorsomedial thalamus, right
more than left lingual gyrus, brainstem (PPN/LTD and tectum), left cerebellar hemisphere lobule VI, left
cerebellar crus I, left more than right superior and left middle cerebellar peduncles, and nodulus (Figure
6, Table 2). Absent were the gyrus rectus, cingulum, operculum, insula, inferior temporal lobes, parietal
and visual cortex, flocculus, vermis, and flocculus. The extent of correlated topography was substantially

1
2 less compared to the anticipatory postural control and reactive postural control sub-score correlations.
3
4 Peak cluster analysis findings (non-corrected at $P < 0.001$) are shown in Supplemental Table 5. Most
5
6 extensive clusters were centered around the bilateral hippocampi, left caudate nucleus and right thalamus
7
8 regions.
9

10 Discussion

11
12
13 Our analysis of four MiniBESTest sub-scores demonstrated shared and unique variance. Whereas the
14
15 MiniBESTest subscores share a portion of variance with each other, each subscore still carries a distinct
16
17 portion of variance that is not explained by the others. Our partial correlation analysis of the MiniBESTest
18
19 domain subscores appears to suggest that anticipatory postural control plays a more central role in dynamic
20
21 balance and gait impairments in PD than previously recognized, as it was the only domain which was
22
23 independently predictive of every other MiniBESTest domain in our sample of patients. A prior
24
25 longitudinal study of gait and balance deficit progression in PD demonstrated that the most pronounced
26
27 longitudinal decline in MiniBESTest total scores was observed among patients with freezing of gait and
28
29 was largely driven by decreases in the anticipatory postural control domain subscore.²⁷ Longitudinal
30
31 emergence of freezing of gait, on the other hand, was associated with specific declines in sensory and
32
33 dynamic gait subscores,²⁷ which we observed were significantly associated with each another and the
34
35 anticipatory domain subscore, but not the reactive domain subscore. The results of our partial correlation
36
37 analysis in conjunction with prior work on longitudinal progression of MiniBESTest scores suggest that
38
39 anticipatory postural control impairments might represent an advanced stage of gait and balance decline
40
41 in PD patients, which would explain why patients with lower anticipatory domain subscores tended to
42
43 have a more severe impairment in all the other domains also.

44
45 We investigated the uncharted territory of cholinergic system changes associating with
46
47 impairments on dynamic gait and balance in individuals with PD, assessed using the MiniBESTest.
48
49 Leveraging the precision of [¹⁸F]-FEOBV, a highly selective radiotracer, we uncovered extensive multi-
50
51 regional correlations between [¹⁸F]-FEOBV binding and both the overall Mini-BESTest scores and its
52
53 functional domain sub-scores. Our findings signify a broader neural network involvement beyond the
54
55 traditionally established regions associated solely with postural control and gait dynamics. Intriguingly,
56
57 we observed correlations within brain regions not conventionally linked to these functions, including the
58
59 right antero-mesofrontal regions, right temporal pole, bilateral fimbria, insula, right cerebellar hemisphere
60
lobule VI, and left cerebellar crus I. Such diverse correlations suggest a more intricate interplay

1
2 contributing to the comprehensive motor impairments observed in PD. The following discussion will
3 comprehensively detail both the shared and distinct correlations across total Mini-BESTest scores and
4 functional domain sub-scores, contextualizing these findings within the landscape of previous studies.
5

6
7 Some regional correlations were found across most of the Mini-BESTest subtests, including
8 medial prefrontal cortex, cingulum, gyrus rectus, insula, right frontotemporal operculum, bilateral
9 mesiotemporal lobes, right temp pole, caudate nucleus, metathalami, thalami proper, brainstem, and some
10 cerebellar regions, such as the right cerebellar hemispheric lobule VI, right flocculus, nodulus, and
11 superior cerebellar peduncles. This pattern is enriched in limbocortical and paralimbic cortical regions,
12 caudate nuclei, metathalami, thalami, and specific cerebellar regions. This pattern also implicates
13 degeneration and/or dysfunction of virtually all brain cholinergic systems in dynamic balance and deficits
14 in PD and further highlights the use of the MiniBESTest as a unidimensional assessment for dynamic gait.
15 The limbic and paralimbic deficits may explain the role of the cholinergic forebrain in modulating
16 incoming sensory information related to dynamic postural control and gait functions,²⁸ since these regions
17 are known to receive extensive cholinergic projections from the basal forebrain Ch4 complex, while also
18 being a major source of reciprocal projections back to the nucleus basalis of Meynert.²⁹ Striatal
19 cholinergic innervation is dominated by striatal cholinergic interneurons, critical for integrating cortically
20 derived sensory information.³⁰ Thalamus and metathalamus receive cholinergic inputs from the
21 pedunculopontine - laterodorsal tegmental complex,³¹ which may serve as a rapid, alerting channel for
22 salient stimuli,³² and cerebellar cholinergic innervation derives heavily from the vestibular complex,³³
23 another critical node for dynamic postural and gait functions.
24
25
26
27
28
29
30
31
32
33
34
35

36
37 These results are consistent with prior work. We previously showed that cholinergic deficits of the
38 metathalamus (lateral geniculate nucleus and medial geniculate nucleus) associate with non-episodic
39 postural control deficits (postural imbalance) as well as episodic mobility disturbances, such as falls and
40 freezing of gait.^{8,9,34} Cholinergic terminal deficits in the cingulum correlated robustly with anticipatory
41 postural control (more posterior cingulum) and reactive postural control (more anterior cingulum). The
42 cingulum is part of a centro-cingulate network that we previously described associated with cognitive
43 deficits in early PD.³⁵ Our cumulative data suggest that cingulum cholinergic afferents may play a role in
44 rapid information exchange in both inter-hemispheric and anterior-to-posterior brain communications that
45 are important in neural circuitry underlying anticipatory postural control and reactive postural control
46 functions in PD. The mesiotemporal limbic cortex, including the hippocampus and its fimbria, is known
47 for its role in spatial navigation - crucial for ambulation.³⁶ We previously also reported a robust association
48 between cholinergic deficits in entorhinal cortex and postural control deficits in PD.⁹
49
50
51
52
53
54
55
56
57
58
59
60

1
2 The insular cortex is an important hub for integration of visceral, emotional, motor, and cognitive
3 information.³⁷ Tinaz *et al.* argued that the insular cortex is an important node for integrating limbic circuit
4 information with basal ganglia motor circuitry.³⁷ Our findings are consistent with this model. The anterior
5 insula also participates in the salience network function where it contributes to bottom-up control of
6 attentional function and flexible transitioning between brain network states³⁸ – cognitive faculties which
7 underpin the adaptive control of behavior in uncertain and constantly changing environments.
8

9
10 Consistent with our prior studies of falls and non-episodic imbalance functions in PD,^{8,9} we found
11 that the cholinergic terminal deficits of the caudate nucleus, as opposed to the putamen, correlated with
12 all Mini-BESTest sub-tests except dynamic gait in this study. Microdialysis work in rats suggests that
13 muscarinic cholinergic signalling in the caudate nucleus is necessary for suppression of old stimulus-
14 response contingencies while new ones are being acquired, a cognitive faculty referred to as “reversal
15 learning”.³⁹ Impaired reversal learning under probabilistic-reward behavioral paradigm has been previously
16 reported in PD patients.⁴⁰ If adaptation of postural control strategy to novel, challenging environmental
17 conditions depends on a process of suppressing old sensory-motor representations while new ones are
18 being actively acquired and engaged (essentially reversal learning), then it might explain why loss of
19 cholinergic signalling in the caudate nucleus appears to play a central role in postural control impairments
20 of PD.
21

22
23 Our study showed evidence of some cholinergic deficits in brainstem subregions, notably the PPN-
24 LDT and tectum. Superior collicular and inferior collicular deficits may reflect degeneration of highly
25 collateralized PPN-LDT projections also innervating the lateral geniculate nucleus and medial geniculate
26 nucleus, respectively.³¹
27

28
29 Our analysis revealed that the regional correlations observed in Mini-BESTest subtest scores were
30 essentially embedded within the broader pattern of correlated deficits identified in the correlation map
31 associated with the Mini-BESTest total score. Interestingly, several regions correlating with specific
32 subtests had been previously recognized as crucial components within the circuits governing various facets
33 of dynamic gait and postural control. For instance, we found a notable association between lower
34 cholinergic nerve terminal integrity in the anterior section of the dorsomedial prefrontal cortex
35 (specifically, upper medial BA 10 and BA 9) and the reactive postural control and sensory orientation
36 subtests. Notably, the medial prefrontal cortex serves as a central hub within significant large-scale neural
37 networks, such as the default mode network, of which the cholinergic basal forebrain is another more
38 recently recognized hub.⁴¹ The topography of gait and balance related cholinergic deficits observed in the
39 present work appears to overlap with two distinct, but closely related, patterns of cerebello-frontal
40 connectivity previously described in the literature: the motor loop, which links together motor cortex,
41
42
43
44
45
46
47
48
49
50
51
52
53
54
55
56
57
58
59
60

1
2 thalamus, and anterior cerebellum, and the executive loop, which connects prefrontal cortex, pons, and
3
4 posterior cerebellum.⁴²
5

6 7 **Anticipatory postural control**

8
9
10 Anticipatory postural adjustments are important components of postural control that prepare for
11 subsequent potentially destabilizing voluntary movements, such as gait initiation. This preparatory phase
12 entails a lateral and posterior shift of the center of mass towards the stance leg followed by a forward shift
13 towards the intended direction of movement,⁴³ and is thought to be mediated by an interaction of primary
14 and supplementary motor cortices with brainstem locomotor centers, including the mesencephalic
15 locomotor region.⁴⁴ Anticipatory postural adjustment modulation is linked to the descending
16 mesencephalic locomotor region pathways to the spinal central pattern generators that are in part
17 controlled by the striatum and cortex.⁴⁴ Our findings align with this understanding, revealing a correlation
18 between brainstem activity and anticipatory postural control sub-scores.
19
20
21
22
23
24
25

26 27 **Reactive postural control**

28
29
30 Reactive postural control is the ability to recover from an unexpected external perturbation to a stable
31 position. Ultimately, reactive postural control determines whether a person will recover from a
32 perturbation or will fall. Bilateral putamina, cerebellum, including the upper anterior cerebellar lobe,
33 vermis and lobule VI, thalamus, and cortical regions (especially the supplemental motor area, paracentral
34 lobule, motor cortex, superior temporal gyrus, and to variable degrees the inferior frontal cortex, anterior
35 prefrontal cortex, insulae, visual cortex, anterior and mid cingulum, fusiform gyrus have been implicated
36 in reactive postural control in fMRI studies.⁴⁵
37
38
39
40
41
42

43 44 **Dynamic gait**

45
46 The MiniBESTest dynamic gait score includes various challenged gait conditions, including changes in
47 gait speed while walking, with head turn, walk with pivot turns, step over obstacles and single and dual
48 Timed Up & Go tests.²² MRI and PET activations of dynamic balance conditions have shown variable
49 involvement of the cerebellum, including the anterior and posterior, vermis, midbrain (red nucleus,
50 mesencephalic locomotor region and pons), thalamus, caudate, putamen, insula, and supplemental motor
51 area, dorsal premotor cortex, and mid cingulum for dynamic balance conditions, including tandem and
52 unipedal stance.⁴⁵
53
54
55
56
57
58
59
60

Sensory orientation

Adaptive control of posture and gait relies on effective multisensory integration of afferent sensory signals originating from visual, somatosensory, and vestibular systems (among other), which occurs across multiple levels of the sensory-motor neural processing hierarchy.⁴⁶ Relatively more automatic walking is less involved with supratentorial locomotor circuitry and depends largely on descending projections from the brainstem to the spinal cord, which include reticulospinal pathways originating from the lateral part of the mesopontine tegmentum.⁴⁴ In contrast, walking in unfamiliar or environmentally more challenging conditions require more cognitive processing of postural control and gait, which depends on knowledge of self-body, such as body schema and body motion in space.⁴⁴ Though the thalamus is primarily known for its role in the relay of sensory information to downstream structures, its contributions to early multi-sensory integration of posture related signals are becoming increasingly recognized.^{10,46,47} Structural integrity of the hippocampus in healthy older adults has been associated with effective postural control under conditions which depend on effective vestibular-proprioceptive integration.⁴⁸ A study on motor imagery of stance was performed on blind and vestibularly-deprived participants, and appeared to suggest the differential involvement of the anterior hippocampal activity in processing of posture-related vestibular information while parahippocampal and fusiform gyrus activity was more strongly implicated in the processing of posture-related visual information.⁴⁹ The hippocampus thus seems to play a role in neural processes related to multisensory balance control. Lastly, higher-order sensory integration mechanisms which support the processing of self-location and first-person perspective appear to depend on multi-modal temporo-parietal cortices.⁵⁰ The sensory orientation sub-test does involve elements of vestibular sensory conflict tested that previously had robust correlations with cholinergic losses in the medial geniculate nucleus.⁵¹ There is recent evidence that projections of the inferior colliculus in the tectum to the medial geniculate nucleus (and other regions) may play a role in alternative relatively spared motor resilience pathways in PD, such as can be seen with paradoxical akinesia.⁵² Other prominently correlated brain regions associated with sensory orientation included the left anterior part of the dorsomedial prefrontal cortex (upper medial BA 10 and BA 9), right more than left dorsolateral prefrontal cortex (BA 8 and 9), bilateral hippocampi, fimbriae, left caudate nucleus, right more than left lateral geniculate nucleus and left medial geniculate nucleus, left dorsomedial thalamus, right more than left lingual gyrus, brainstem, nodulus, left cerebellar lobule VI and left crus I, left more than right superior cerebellar peduncles and left middle cerebellar peduncle.

Our findings present compelling evidence indicating cholinergic deficits in brain regions not conventionally linked to postural control and dynamic gait functions. Specifically, we observed

1 correlation with the right antero-mesofrontal regions, right temporal pole, bilateral fimbria, insula, right
2 cerebellar hemisphere lobule VI, and left cerebellar crus I. These areas, although not traditionally
3 associated with gait and balance, might play a significant role in orchestrating motor functions within the
4 broader spectrum of PD. The involvement of these seemingly unrelated regions underscores the intricate
5 and widespread impact of cholinergic deficits on motor control in PD. This suggests a broader neural
6 network involvement beyond the established regions directly linked to postural control and gait dynamics.
7 The aberrations detected in these regions might contribute to the comprehensive motor impairments
8 witnessed in PD, shedding new light on the multifaceted nature of motor dysfunction in this condition.
9 Plus, these results underscore the importance of employing highly specific radiotracers, like [¹⁸F]-
10 FEOBV. Coupled with a comprehensive evaluation of gait and balance, the use of such precise imaging
11 tools becomes imperative to unravel the complex and nuanced role of cholinergic dysfunction in these
12 clinical manifestations within PD. The involvement of these seemingly unrelated regions highlights the
13 need for a more holistic understanding of the neural underpinnings of motor dysfunction in PD, urging a
14 broader exploration beyond established motor control regions.
15

16 An unexpected finding in our study was that cholinergic deficits of the right temporal pole were
17 robustly associated with anticipatory postural and reactive postural control. It is possible that connectivity
18 with the hippocampus and processing of emotional information may play a role.⁵³

19 The vestibular system and its cerebellar connections play critical roles in dynamic gait and postural
20 functions. Medial vestibular cholinergic neurons are important inputs to the vestibular cerebellum.³³
21 Cerebellar cholinergic deficits in this study were variable across the spectrum of the vestibular cerebellum
22 (flocculus, nodulus) with correlated impairments in anticipatory postural control, reactive postural control
23 and sensory orientation. We also found evidence of correlated cholinergic deficits in cerebellar cortical
24 regions. Cerebellar regions included the flocculus, upper vermis and the hemispheric regions. The
25 involvement flocculus and vermis may reflect vestibular and proprioceptive sensory information
26 processing, respectively.⁵⁴ The flocculus is known to contribute to the vestibulo-ocular reflex which
27 stabilizes gaze during head rotation.⁵⁵ We found that the right flocculus had significant association with
28 reactive postural control alone. The orienting eye velocity of the slow component of the angular vestibulo-
29 ocular reflex also crucially depends on the nodulus and rostral-ventral uvula of the vestibulo-cerebellum
30 function.⁵⁶

31 Associations with the upper vermis region were present for anticipatory postural control and
32 reactive postural control. This may be in part associated with the cerebellar locomotor region.⁴⁴ Cerebellar
33 lobule VI has been implicated as part of neural circuitry involved in spatial and sensorimotor processing.⁵⁷
34 We found evidence that cholinergic lobule VI changes are associated with reactive postural control,
35

1
2 dynamic gait, and sensory orientation in the PD population. Cerebellar lobule VI and crus I may also play
3 a role in visual divergent thinking.⁵⁸ Crus I has also been found to be involved with emotional processing
4 implicating cerebellar-limbic circuitry that may be activated with fear of falling in persons with PD and
5 falls.⁵⁹
6
7

8
9 The wide range of correlated cholinergic deficits, involving all major brain cholinergic systems, is
10 intriguing. It is possible that this reflects redundancy in brain systems underpinning dynamic balance
11 functions. Dysfunction of multiple systems-regions may be needed to markedly disrupt these important
12 functions. Our results imply potential avenues for pharmacologic therapies targeting cholinergic deficits,
13 offering promise for future intervention strategies. Our findings may also support research into novel
14 approaches for the management of dynamic balance and gait changes in PD, including targeting novel
15 cholinergic regions involved in dynamic balance and gait with invasive or non-invasive neurostimulation
16 techniques.
17
18

19 We also found that the extent of involved cholinergic topography was substantially less
20 pronounced for the sensory orientation sub-test compared to the anticipatory and reactive postural control
21 Mini-BESTest sub-scores and did not survive whole brain correction for multiple testing. We conclude
22 that specific dynamic balance and gait deficits are associated with overlapping but also distinct patterns
23 of cerebral cholinergic system changes in widespread brain regions in PD. This is a unique study as this
24 study shows evidence of *novel patterns* of cholinergic deficits involved in dynamic balance and gait
25 disruption in PD, including the right temporal pole, right anterior part of the dorsomedial prefrontal cortex,
26 gyrus rectus, fimbriae, lingual gyrus, cerebellar peduncles, right lobules VI and left crus I, flocculus, and
27 nodulus. Despite substantial cholinergic topographic overlap between anticipatory and reactive postural
28 control subscores our clinicometric analysis demonstrated that anticipatory but not reactive postural control
29 sub-score is a major determinant of dynamic balance and gait in Parkinson's disease.
30
31

32 There are several limitations of this study including its cross-sectional analysis design, which
33 precludes us from making inferences about the relationship between the trajectory of cholinergic system
34 decline and disease progression. PET imaging was performed in the dopaminergic medication 'on' state,
35 which arguably might have influenced our result, though our prior work shows that dopamine D2 receptor
36 agonist intake, which was also associated with ~500 mg higher levodopa equivalent dose on average, did
37 not appear to correlate significantly with [¹⁸F]-FEOBV binding in PD patients scanned in 'on' state.⁶⁰
38 Furthermore, the statistical parametric mapping approaches we applied herein included levodopa
39 equivalent dose as a covariate, to control for its possible influence on the FEOBV signal. Lastly, due to
40 the limitations of the [¹⁸F]-FEOBV, we can only make inference about the density of pre-synaptic nerve
41 terminals, and not about any specific muscarinic/nicotinic post-synaptic cholinergic signalling targets
42
43
44
45
46
47
48
49
50
51
52
53
54
55
56
57
58
59
60

1
2 engaged by these nerve terminals, which would require other radioligands or pharmaceutical interventions
3 specifically targeting these receptors.
4

5 6 **Acknowledgments**

7
8
9
10 The authors thank our study coordinators, the PET technologists, cyclotron operators, and chemists, for their
11 assistance. We are indebted to the subjects who participated in this study.
12

13 14 **Funding**

15
16
17
18 This study was funded by National Institutes of Health (R01 AG073100, P01 NS015655, RO1 NS070856,
19 P50 NS091856, P50 NS123067), Department of Veterans Affairs grant (I01 RX001631), the Michael J. Fox
20 Foundation, and the Parkinson's Foundation. None of the funding agencies had a role in the design and
21 conduct of the study, in the collection, management, analysis and interpretation of the data, in the
22 preparation, review or approval of the manuscript, nor in the decision to submit the manuscript for
23 publication.
24
25
26
27

28 29 **Data availability**

30
31
32 All data are available upon reasonable request.
33
34

35 36 **Competing Interests**

37
38
39 The authors report no competing interests and that the research was conducted in the absence of any
40 commercial or financial relationships that could be construed as a potential conflict of interest.
41
42
43
44
45
46
47
48
49
50
51
52
53
54
55
56
57
58
59
60

References

1. Muslimović D, Post B, Speelman JD, Schmand B, de Haan RJ. Determinants of disability and quality of life in mild to moderate {Parkinson} disease. *Neurology*. 2008;70(23):2241-2247.
2. Schrag A, Hovris A, Morley D, Quinn N, Jahanshahi M. Caregiver-burden in {Parkinson}'s disease is closely associated with psychiatric symptoms, falls, and disability. *Parkinsonism Relat Disord*. 2006;12(1):35-41.
3. Müller MLTM, Marusic U, van Emde Boas M, Weiss D, Bohnen NI. Treatment options for postural instability and gait difficulties in {Parkinson}'s disease. *Expert Rev Neurother*. 2019;19(12):1229-1251.
4. López IC, Ruiz PJG, Del Pozo SVF, Bernardos VS. Motor complications in {Parkinson}'s disease: {Ten} year follow-up study. *Mov Disord*. 2010;25(16):2735-2739.
5. Vu TC, Nutt JG, Holford NHG. Progression of motor and nonmotor features of {Parkinson}'s disease and their response to treatment. *Br J Clin Pharmacol*. 2012;74(2):267-283.
6. Curtze C, Nutt JG, Carlson-Kuhta P, Mancini M, Horak FB. Levodopa {I} sa {D} ouble- $\{E\}$ dged {S} word for {B} alance and {G} ait in {P} eople {W} ith {P} arkinson's {D} isease. *Mov Disord*. 2015;30(10):1361-1370.
7. Bohnen NI, Müller MLTM, Koeppe RA, et al. History of falls in Parkinson disease is associated with reduced cholinergic activity. *Neurology*. 2009;73(20):1670-1676. doi:10.1212/WNL.0b013e3181c1ded6
8. Bohnen NI, Kanel P, Zhou Z, et al. Cholinergic system changes of falls and freezing of gait in Parkinson's disease. *Ann Neurol*. 2019;85(4):538-549.
9. Bohnen NI, Kanel P, Koeppe RA, et al. Regional cerebral cholinergic nerve terminal integrity and cardinal motor features in {Parkinson}'s disease. *Brain Commun*. 2021;3(2):fcab109.
10. Müller MLTM, Albin RL, Kotagal V, et al. Thalamic cholinergic innervation and postural sensory integration function in {Parkinson}'s disease. *Brain*. 2013;136(11):3282-3289.
11. Roytman S, Paalanen R, Griggs A, et al. Cholinergic system correlates of postural control changes in {Parkinson}'s disease freezers. *Brain*. Published online 2023:awad134.
12. Albin RL, Bohnen NI, Muller MLTM, et al. Regional vesicular acetylcholine transporter distribution in human brain: a [18F] fluoroethoxybenzovesamicol positron emission tomography study. *J Comp Neurol*. 2018;526(17):2884-2897.

13. Leddy AL, Crowner BE, Earhart GM. Utility of the {Mini}-{BESTest}, {BESTest}, and {BESTest} sections for balance assessments in individuals with {Parkinson} disease. *J Neurol Phys Ther JNPT*. 2011;35(2):90.
14. Franchignoni F, Godi M, Corna S, Giordano A. Rasch validation of the {Mini}-{BESTest} in people with {Parkinson} disease. *J Neurol Phys Ther*. 2022;46(3):219-226.
15. King LA, Priest KC, Salarian A, Pierce D, Horak FB. Comparing the {Mini}-{BESTest} with the {Berg} {Balance} {Scale} to evaluate balance disorders in {Parkinson}'s disease. *Park Dis*. 2012;2012.
16. Leavy B, Joseph C, Löfgren N, Johansson H, Hagströmer M, Franzén E. Outcome evaluation of highly challenging balance training for people with {Parkinson} disease: a multicenter effectiveness-implementation study. *J Neurol Phys Ther*. 2020;44(1):15-22.
17. Lopes LKR, Scianni AA, Lima LO, de Carvalho Lana R, Rodrigues-De-Paula F. The {Mini}-{BESTest} is an independent predictor of falls in {Parkinson} {Disease}. *Braz J Phys Ther*. 2020;24(5):433-440.
18. Hughes AJ, Daniel SE, Kilford L, Lees AJ. Accuracy of clinical diagnosis of idiopathic Parkinson's disease: a clinico-pathological study of 100 cases. *J Neurol Neurosurg Psychiatry*. 1992;55(3):181-184.
19. Goetz CG, Fahn S, Martinez-Martin P, et al. Movement {Disorder} {Society}-sponsored revision of the {Unified} {Parkinson}'s {Disease} {Rating} {Scale} ({MDS}-{UPDRS}): process, format, and clinimetric testing plan. *Mov Disord*. 2007;22(1):41-47.
20. Nasreddine ZS, Phillips NA, Bédirian V, et al. The Montreal Cognitive Assessment, MoCA: a brief screening tool for mild cognitive impairment. *J Am Geriatr Soc*. 2005;53(4):695-699.
21. Tomlinson CL, Stowe R, Patel S, Rick C, Gray R, Clarke CE. Systematic review of levodopa dose equivalency reporting in Parkinson's disease. *Mov Disord*. 2010;25(15):2649-2653.
22. Franchignoni F, Horak F, Godi M, Nardone A, Giordano A. Using psychometric techniques to improve the {Balance} {Evaluation} {System}'s {Test}: the mini-{BESTest}. *J Rehabil Med Off J UEMS Eur Board Phys Rehabil Med*. 2010;42(4):323.
23. Shao X, Hoareau R, Hockley BG, et al. Highlighting the versatility of the tracerlab synthesis modules. {Part} 1: fully automated production of [{18F}] labelled radiopharmaceuticals using a {Tracerlab} {FXFN}. *J Label Compd Radiopharm*. 2011;54(6):292-307.
24. Petrou M, Frey KA, Kilbourn MR, et al. In vivo imaging of human cholinergic nerve terminals with (-)-5-18F-fluoroethoxybenzovesamicol: biodistribution, dosimetry, and tracer kinetic analyses. *J Nucl Med*. 2014;55(3):396-404. doi:10.2967/jnumed.113.124792
25. Aghourian M, Legault-Denis C, Soucy JP, et al. Quantification of brain cholinergic denervation in Alzheimer's disease using PET imaging with [18F]-FEOBV. *Mol Psychiatry*. 2017;22(11):1531-1538. doi:10.1038/mp.2017.183

- 1
2
3 26. Nejad-Davarani S, Koeppe RA, Albin RL, Frey KA, Müller MLTM, Bohnen NI.
4 Quantification of brain cholinergic denervation in dementia with {Lewy} bodies using
5 {PET} imaging with [{18F}]-{FEOBV}. *Mol Psychiatry*. 2019;24(3):322-327.
6
7
8 27. Vervoort G, Bengevoord A, Strouwen C, et al. Progression of postural control and gait
9 deficits in Parkinson's disease and freezing of gait: A longitudinal study. *Parkinsonism Relat*
10 *Disord*. 2016;28:73-79. doi:10.1016/j.parkreldis.2016.04.029
11
12 28. Robertson RT, Kaitz SS, Robards MJ. A subcortical pathway links sensory and limbic
13 systems of the forebrain. *Neurosci Lett*. 1980;17(1-2):161-165. doi:10.1016/0304-
14 3940(80)90078-6
15
16 29. Mesulam MM. The cholinergic innervation of the human cerebral cortex. In: *Progress in*
17 *Brain Research*. Vol 145. Elsevier; 2004:67-78. doi:10.1016/S0079-6123(03)45004-8
18
19 30. Albin RL, van der Zee S, van Laar T, et al. Cholinergic systems, attentional-motor
20 integration, and cognitive control in Parkinson's disease. *Prog Brain Res*. 2022;269(1):345-
21 371. doi:10.1016/bs.pbr.2022.01.011
22
23 31. Huerta-Ocampo I, Hacioglu-Bay H, Dautan D, Mena-Segovia J. Distribution of Midbrain
24 Cholinergic Axons in the Thalamus. *eneuro*. 2020;7(1):ENEURO.0454-19.2019.
25 doi:10.1523/ENEURO.0454-19.2019
26
27 32. Sarter M, Lustig C. Cholinergic double duty: cue detection and attentional control. *Curr*
28 *Opin Psychol*. 2019;29:102-107. doi:10.1016/j.copsyc.2018.12.026
29
30 33. Jaarsma D, Ruigrok TJH, Caffé R, et al. Chapter 5 Cholinergic innervation and receptors in
31 the cerebellum. In: *Progress in Brain Research*. Vol 114. Elsevier; 1997:67-96.
32 doi:10.1016/S0079-6123(08)63359-2
33
34 34. Bohnen NI, Kanel P, van Emde Boas M, Roytman S, Kerber KA. Vestibular Sensory
35 Conflict During Postural Control, Freezing of Gait, and Falls in Parkinson's Disease. *Mov*
36 *Disord*. 2022;37(11):2257-2262. doi:10.1002/mds.29189
37
38 35. Van Der Zee S, Kanel P, Müller MLTM, Van Laar T, Bohnen NI. Identification of
39 cholinergic centro-cingulate topography as main contributor to cognitive functioning in
40 Parkinson's disease: Results from a data-driven approach. *Front Aging Neurosci*.
41 2022;14:1006567. doi:10.3389/fnagi.2022.1006567
42
43 36. Ruiz NA, Meager MR, Agarwal S, Aly M. The Medial Temporal Lobe Is Critical for Spatial
44 Relational Perception. *J Cogn Neurosci*. 2020;32(9):1780-1795. doi:10.1162/jocn_a_01583
45
46 37. Tinaz S, Para K, Vives-Rodriguez A, et al. Insula as the Interface Between Body Awareness
47 and Movement: A Neurofeedback-Guided Kinesthetic Motor Imagery Study in Parkinson's
48 Disease. *Front Hum Neurosci*. 2018;12:496. doi:10.3389/fnhum.2018.00496
49
50
51
52
53
54
55
56
57
58
59
60

- 1
2
3 38. Peters SK, Dunlop K, Downar J. Cortico-Striatal-Thalamic Loop Circuits of the Salience
4 Network: A Central Pathway in Psychiatric Disease and Treatment. *Front Syst Neurosci.*
5 2016;10. doi:10.3389/fnsys.2016.00104
6
- 7
8 39. Ragozzino ME. Acetylcholine actions in the dorsomedial striatum support the flexible
9 shifting of response patterns. *Neurobiol Learn Mem.* 2003;80(3):257-267.
10 doi:10.1016/S1074-7427(03)00077-7
11
- 12 40. Peterson DA, Elliott C, Song DD, Makeig S, Sejnowski TJ, Poizner H. Probabilistic reversal
13 learning is impaired in Parkinson's disease. *Neuroscience.* 2009;163(4):1092-1101.
14 doi:10.1016/j.neuroscience.2009.07.033
15
- 16 41. Alves PN, Foulon C, Karolis V, et al. An improved neuroanatomical model of the default-
17 mode network reconciles previous neuroimaging and neuropathological findings. *Commun*
18 *Biol.* 2019;2(1):370. doi:10.1038/s42003-019-0611-3
19
- 20 42. Kelly RM, Strick PL. Cerebellar Loops with Motor Cortex and Prefrontal Cortex of a
21 Nonhuman Primate. *J Neurosci.* 2003;23(23):8432-8444. doi:10.1523/JNEUROSCI.23-23-
22 08432.2003
23
- 24 43. Gélât T, Pellec AL, Brenière Y. Evidence for a common process in gait initiation and
25 stepping on to a new level to reach gait velocity. *Exp Brain Res.* 2006;170(3):336-344.
26 doi:10.1007/s00221-005-0214-8
27
- 28 44. Takakusaki K. Functional Neuroanatomy for Posture and Gait Control. *J Mov Disord.*
29 2017;10(1):1-17. doi:10.14802/jmd.16062
30
- 31 45. Dijkstra BW, Bekkers EMJ, Gilat M, De Rond V, Hardwick RM, Nieuwboer A. Functional
32 neuroimaging of human postural control: A systematic review with meta-analysis. *Neurosci*
33 *Biobehav Rev.* 2020;115:351-362. doi:10.1016/j.neubiorev.2020.04.028
34
- 35 46. Roytman S, Paalanen R, Carli G, et al. Multisensory mechanisms of gait and balance in
36 Parkinson's disease: an integrative review. *Neural Regen Res.*:10-4103.
37
- 38 47. Zwergal A, La Fougère C, Lorenzl S, et al. Postural imbalance and falls in PSP correlate
39 with functional pathology of the thalamus. *Neurology.* 2011;77(2):101-109.
40 doi:10.1212/WNL.0b013e318223c79d
41
- 42 48. Beauchet O, Barden J, Liu-Ambrose T, Chester VL, Szturm T, Allali G. The relationship
43 between hippocampal volume and static postural sway: results from the GAIT study. *AGE.*
44 2016;38(1):19. doi:10.1007/s11357-016-9883-4
45
- 46 49. Jahn K, Deutschländer A, Stephan T, Strupp M, Wiesmann M, Brandt T. Brain activation
47 patterns during imagined stance and locomotion in functional magnetic resonance imaging.
48 *NeuroImage.* 2004;22(4):1722-1731. doi:10.1016/j.neuroimage.2004.05.017
49
50
51
52
53
54
55
56
57
58
59
60

- 1
2
3 50. Ionta S, Heydrich L, Lenggenhager B, et al. Multisensory Mechanisms in Temporo-Parietal
4 Cortex Support Self-Location and First-Person Perspective. *Neuron*. 2011;70(2):363-374.
5 doi:10.1016/j.neuron.2011.03.009
6
7
8 51. Bohnen NI, Kanel P, Roytman S, et al. Cholinergic brain network deficits associated with
9 vestibular sensory conflict deficits in Parkinson's disease: correlation with postural and gait
10 deficits. *J Neural Transm*. 2022;129(8):1001-1009.
11
12 52. Melo-Thomas L, Schwarting RKW. Paradoxical kinesia may no longer be a paradox waiting
13 for 100 years to be unraveled. *Rev Neurosci*. 2023;34(7):775-799. doi:10.1515/revneuro-
14 2023-0010
15
16 53. Setton R, Sheldon S, Turner GR, Spreng RN. Temporal pole volume is associated with
17 episodic autobiographical memory in healthy older adults. *Hippocampus*. 2022;32(5):373-
18 385. doi:10.1002/hipo.23411
19
20 54. Cullen KE. Internal models of self-motion: neural computations by the vestibular
21 cerebellum. *Trends Neurosci*. 2023;46(11):986-1002. doi:10.1016/j.tins.2023.08.009
22
23 55. Belton T, McCrea RA. Role of the Cerebellar Flocculus Region in the Coordination of Eye
24 and Head Movements During Gaze Pursuit. *J Neurophysiol*. 2000;84(3):1614-1626.
25 doi:10.1152/jn.2000.84.3.1614
26
27 56. Cohen B, John P, Yakushin SB, Buettner-Ennever J, Raphan T. The Nodulus and Uvula:
28 Source of Cerebellar Control of Spatial Orientation of the Angular Vestibulo-Ocular Reflex.
29 *Ann N Y Acad Sci*. 2002;978(1):28-45. doi:10.1111/j.1749-6632.2002.tb07553.x
30
31 57. Stoodley C, Schmahmann J. Functional topography in the human cerebellum: A meta-
32 analysis of neuroimaging studies. *NeuroImage*. 2009;44(2):489-501.
33 doi:10.1016/j.neuroimage.2008.08.039
34
35 58. Gao Z, Liu X, Zhang D, Liu M, Hao N. The indispensable role of the cerebellum in visual
36 divergent thinking. *Sci Rep*. 2020;10(1):16552. doi:10.1038/s41598-020-73679-9
37
38 59. Baumann O, Mattingley JB. Cerebellum and Emotion Processing. In: Adamaszek M, Manto
39 M, Schutter DJLG, eds. *The Emotional Cerebellum*. Vol 1378. Advances in Experimental
40 Medicine and Biology. Springer International Publishing; 2022:25-39. doi:10.1007/978-3-
41 030-99550-8_3
42
43 60. Albin RL, Kanel P, van Laar T, et al. No dopamine agonist modulation of brain [18F]
44 FEOBV binding in parkinson's disease. *Mol Pharm*. 2022;19(4):1176-1182.
45
46
47
48
49
50
51
52
53
54
55
56
57
58
59
60

Figure legends

Figure 1. Summary of Mini-BESTest assessments

Figure 2. Whole brain vesicular acetylcholine transporter PET voxel-based correlation analysis and total Mini-BESTest scores.

Whole brain voxel-based correlation analysis t-value statistic image (N = 125, FDR-corrected, $P < 0.05$) for total Mini-BESTest scores included the following vesicular acetylcholine transporter binding regions: gyrus rectus, orbitofrontal regions, right anterior dorsomedial prefrontal cortex (upper medial BA 10 and BA 9), bilateral dorsolateral prefrontal cortex, all segments of the cingulum, bilateral insula, right more than left frontotemporal operculum, bilateral mesiotemporal cortex, left mid posterior temporal cortex, right more than left fimbriae/isthmus cingulum, right temporal pole, bilateral caudate nuclei, metathalami (lateral and medial geniculate bodies), thalami proper, right parietal cortex, left more than right peri-central cortex, occipital cortex, right more than left lingual gyri, right cerebellar hemisphere lobule VI, left cerebellar crus I, bilateral superior cerebellar peduncles, nodulus, right flocculus, and upper dorsal vermis. No significant correlations were found for the putamen and anteroventral striatum.

Figure 3. Whole brain vesicular acetylcholine transporter PET voxel-based correlations and anticipatory postural control.

Whole brain statistical non-parametric mapping (SnPM) voxel-based analysis pseudo t-value statistic image showed regionally significant false discovery rate (FDR)-corrected (N = 125, $P < 0.05$) correlations between the Mini-BESTest and anticipatory postural control sub-test scores were seen in the following vesicular acetylcholine transporter binding regions: bilateral gyrus rectus, bilateral orbitofrontal regions, anterior cingulum, bilateral dorsolateral prefrontal cortex (BA 8 & 9), right more than left frontotemporal operculum, right insula, bilateral fimbriae/isthmus cingulum, right temporal pole, bilateral caudate nuclei, lateral and medial geniculate bodies, thalami proper, bilateral occipital cortex, right more than left lingual gyri, left precentral cortex, brainstem (mesencephalic tectum), right cerebellar hemisphere lobule VI, bilateral superior cerebellar peduncles, nodulus, and upper dorsal vermis. No significant correlations were seen for the putamen, anteroventral striatum, right parietal cortex, and the flocculus.

1
2
3 **Figure 4. Whole brain vesicular acetylcholine transporter PET voxel-based correlations and**
4 **reactive postural control.**
5

6
7
8 Whole brain statistical non-parametric mapping (SnPM) voxel-based analysis pseudo t-value
9 statistic image showed regionally significant FDR-corrected ($N = 125$, $P < 0.05$) correlations
10 between vesicular acetylcholine transporter PET and the reactive postural control sub-tests scores
11 in the bilateral gyrus rectus, bilateral orbitofrontal cortex, right more than left anterior parts of the
12 dorsomedial prefrontal cortex (upper medial BA 10 and BA 9), bilateral dorsolateral prefrontal
13 cortex (BA 8 & 9), anterior cingulum, left more than right frontotemporal operculum, bilateral
14 insula, bilateral mesiotemporal lobes, bilateral fimbriae/isthmus cingulum, left peri-central cortex,
15 right temporal pole, inferior temporal lobes, left mid and posterior temporal lobe, bilateral caudate
16 nuclei, lateral and medial geniculate nuclei, left pulvinar, right parietal cortex, right flocculus,
17 nodulus, bilateral superior cerebellar peduncles. Notably absent were the putamen, anteroventral
18 striatum, right cerebellar lobule VI, brainstem, and visual cortex.
19
20
21
22
23
24
25
26

27 **Figure 5. Dynamic gait scores.**
28

29
30 Exploratory statistical non-parametric mapping (SnPM) whole brain voxel-based analysis pseudo
31 t-value statistic image ($N = 125$, non-corrected at $P = 0.001$) showed correlations between the
32 dynamic gait scores and vesicular acetylcholine transporter expression in the right dorsolateral
33 prefrontal cortex (BA 8 & 9), right insula, bilateral mesiotemporal, bilateral mid posterior temporal
34 cortex, right fimbriae/isthmus cingulum, right lateral geniculate nucleus, bilateral superior thalami,
35 brainstem (PPN/LTD and tectum), and right cerebellar hemisphere lobule VI. Notably absent were
36 the gyrus rectus, orbitofrontal regions, cingulum, anteromesial frontal regions, right temporal pole,
37 caudate nuclei, The extent of involved topography was substantially less compared to the
38 anticipatory and reactive postural control Mini-BESTest sub-scores.
39
40
41
42
43
44
45
46

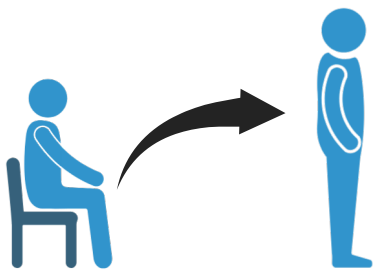
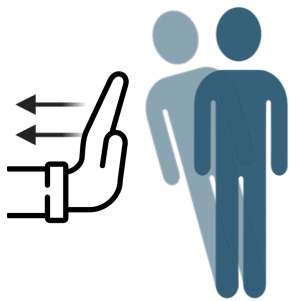
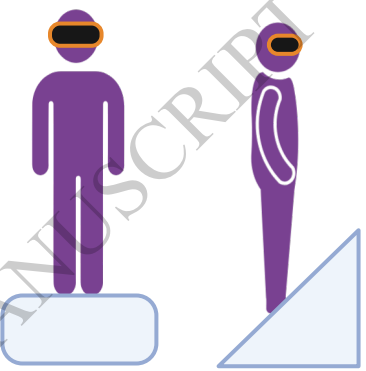
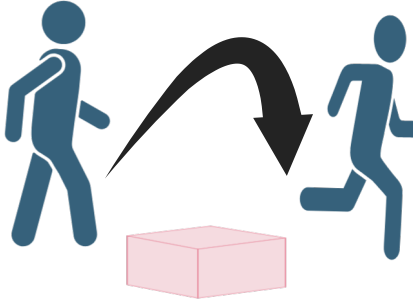
47 **Figure 6. Sensory orientation.**
48

49
50 Exploratory whole brain statistical non-parametric mapping (SnPM) voxel-based analysis pseudo
51 t-value statistic image ($N = 125$, non-corrected at $P = 0.001$) showed regional correlations between
52 the sensory orientation scores and vesicular acetylcholine transporter expression in the left anterior
53 part of the dorsomedial prefrontal cortex (upper medial BA 10 and BA 9), right more than left
54
55
56
57
58
59
60

1
2
3 dorsolateral prefrontal cortex (BA 8 & 9), bilateral hippocampi, bilateral fimbriae/isthmus
4 cingulum, left caudate nucleus, right more than left lateral geniculate nuclei, left medial geniculate
5 nucleus, left dorsomedial thalamus, right more than left lingual gyrus, brainstem (PPN/LTD and
6 tectum), left cerebellar hemisphere lobule VI, left cerebellar crus I, left more than right superior
7 and left middle cerebellar peduncles and nodulus. Notably absent were the gyrus rectus, cingulum,
8 operculum, insula, inferior temporal lobes, parietal and visual cortex, flocculus, vermis, and
9 flocculus.
10
11
12
13
14
15
16
17
18
19
20
21
22
23
24
25
26
27
28
29
30
31
32
33
34
35
36
37
38
39
40
41
42
43
44
45
46
47
48
49
50
51
52
53
54
55
56
57
58
59
60

ACCEPTED MANUSCRIPT

1
2
3
4
5
6
7
8
9
10
11
12
13
14
15
16
17
18
19
20
21
22
23
24
25
26
27
28
29
30
31
32
33
34
35
36
37

Anticipatory postural adjustments Scored: 0-6	Reactive Postural Control Scored: 0-6	Sensory Orientation Scored: 0-6	Dynamic Gait Scored: 0-10
			
Self-initiated change in base of support	Reaction to unexpected perturbation caused by removal of external support	Maintaining balance under different sensory conditions	Maintaining balance during various gait conditions
1) Sit to stand (0-2) 2) Rise to toes (0-2) 3) Stand on one leg left and right (0-2)*	1) Compensatory Stepping Correction Forward (0-2) 2) Compensatory Stepping Correction Backwards (0-2) 3) Compensatory stepping correction lateral (0-2)*	1) Eyes Open Firm Surface (0-2) 2) Eyes Closed Foam Surface(0-2) 3) Eyes Closed Incline (0-2)	1) Change in Gait Speed (0-2) 2) Walk With Head Turns Horizontal (0-2) 3) Walk With Pivot Turns (0-2) 4) Step Over Obstacles 5) Timed Up and Go with Dual Task (3 Meter walk) (0-2)

38 Score determination:
 39 2= Normal
 40 1= Moderate
 41 0= Severe

*Scores are calculated by taking the side left or right with the lowest numerical score

42
43
44

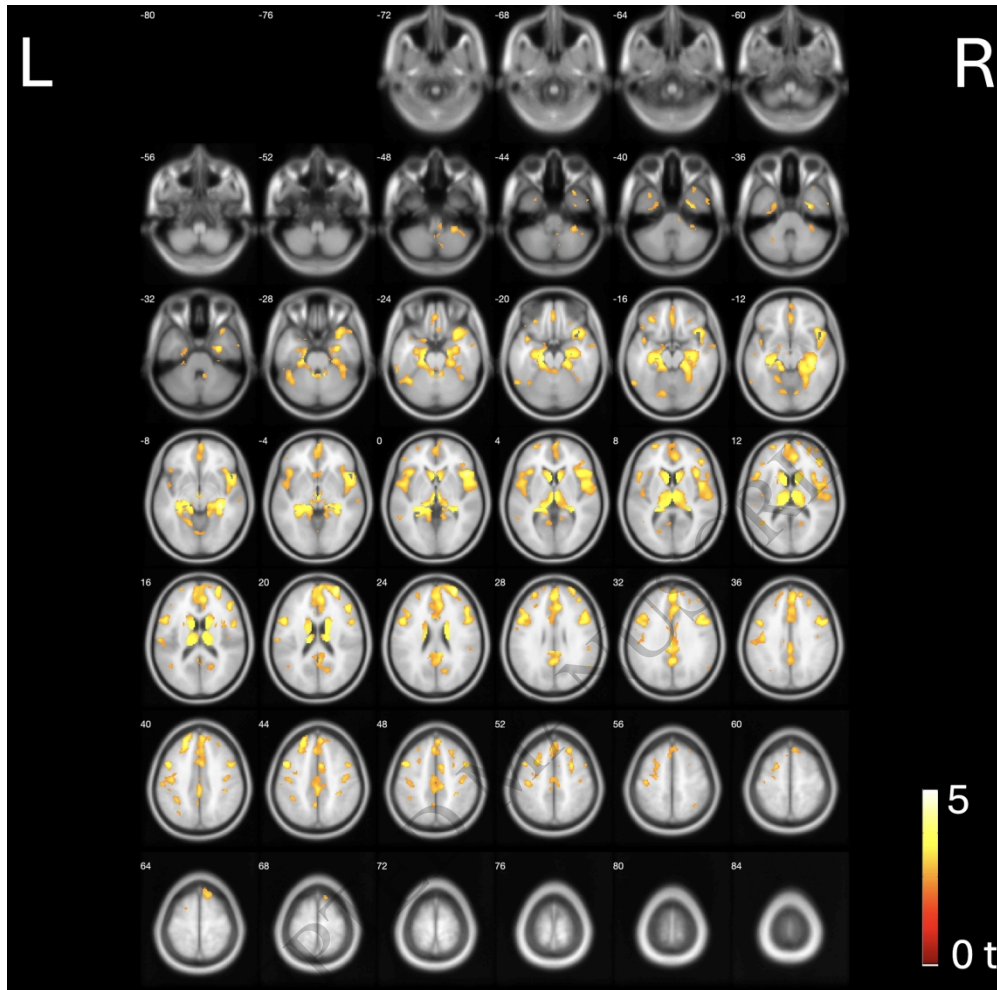


FIGURE 2: Mini-BESTest Total FDR < 0.05

278x274mm (300 x 300 DPI)

ACCEPTED

1
2
3
4
5
6
7
8
9
10
11
12
13
14
15
16
17
18
19
20
21
22
23
24
25
26
27
28
29
30
31
32
33
34
35
36
37
38
39
40
41
42
43
44
45
46
47
48
49
50
51
52
53
54
55
56
57
58
59
60

1
2
3
4
5
6
7
8
9
10
11
12
13
14
15
16
17
18
19
20
21
22
23
24
25
26
27
28
29
30
31
32
33
34
35
36
37
38
39
40
41
42
43
44
45
46
47
48
49
50
51
52
53
54
55
56
57
58
59
60

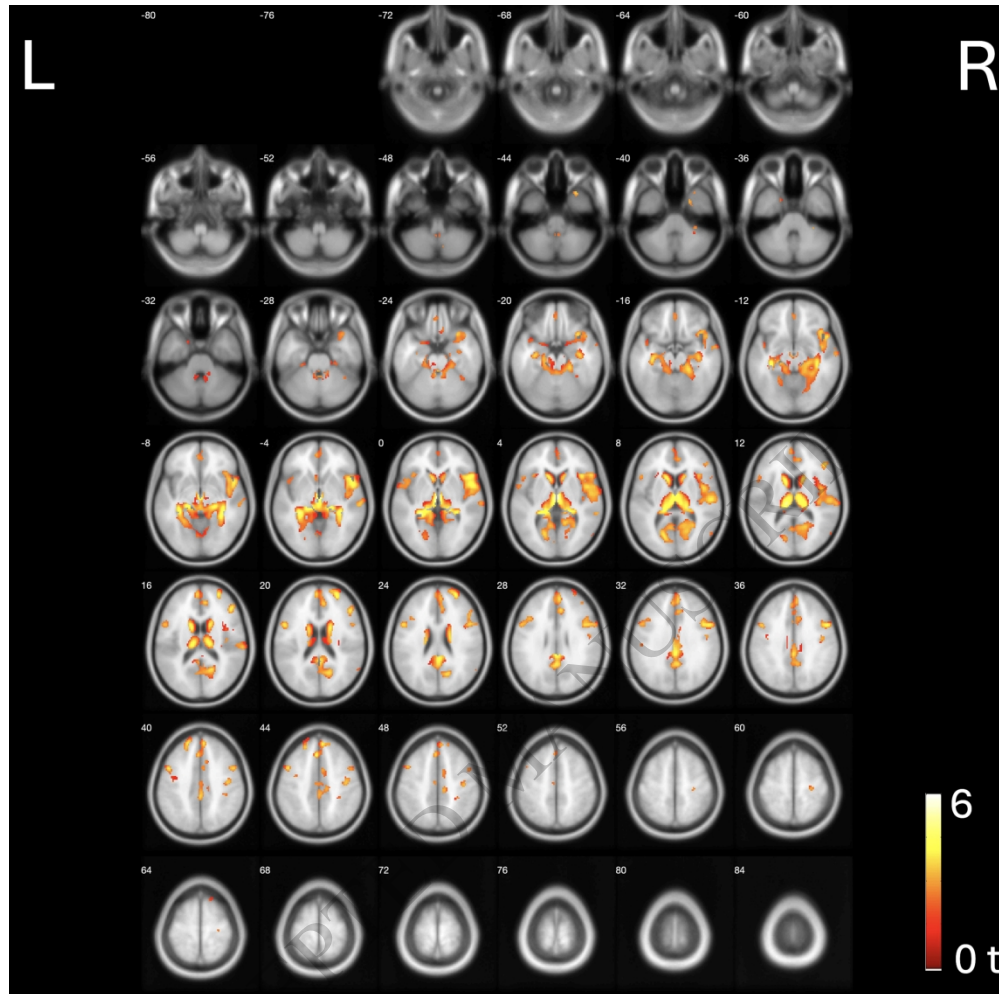


FIGURE 3: Mini-BESTest Anticipatory Postural Control (APC) FDR < 0.05

278x276mm (300 x 300 DPI)

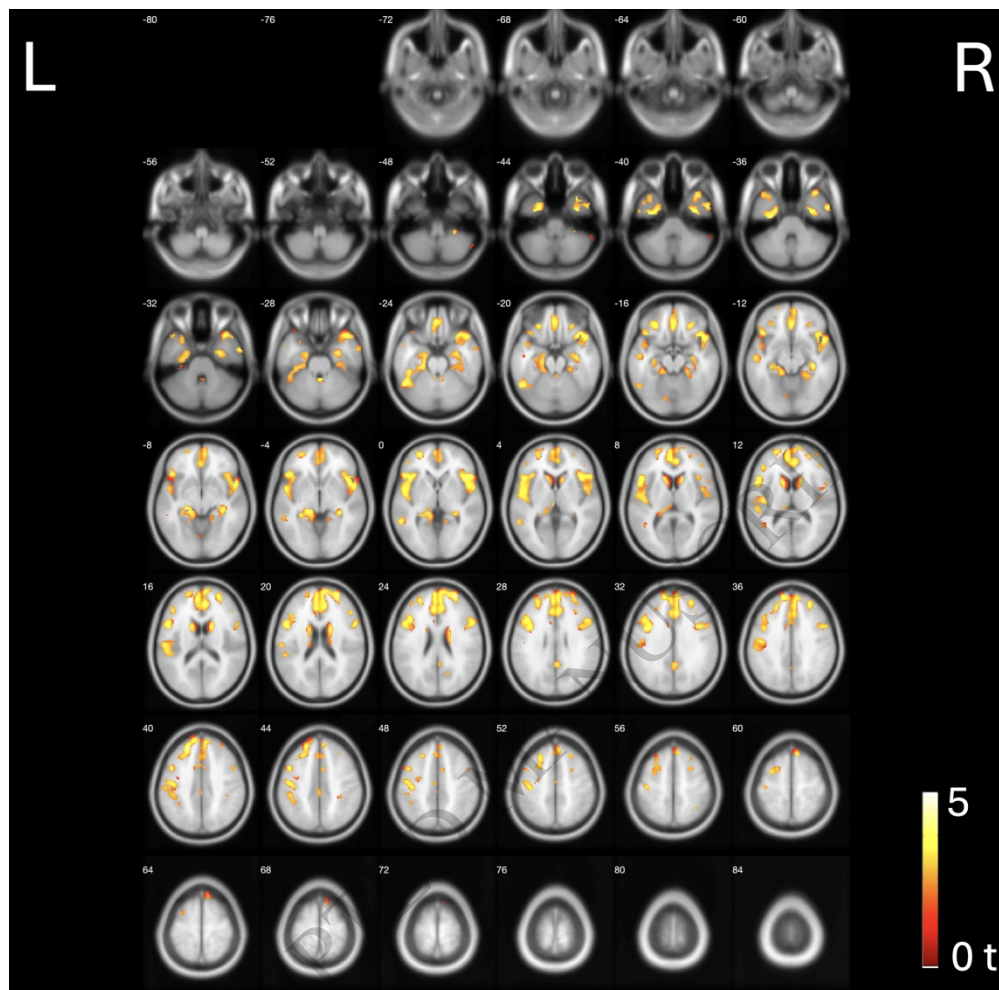


FIGURE 4: Mini-BESTest Reactive Postural Control (RPC) SnPM FDR < 0.05

278x274mm (300 x 300 DPI)

1
2
3
4
5
6
7
8
9
10
11
12
13
14
15
16
17
18
19
20
21
22
23
24
25
26
27
28
29
30
31
32
33
34
35
36
37
38
39
40
41
42
43
44
45
46
47
48
49
50
51
52
53
54
55
56
57
58
59
60

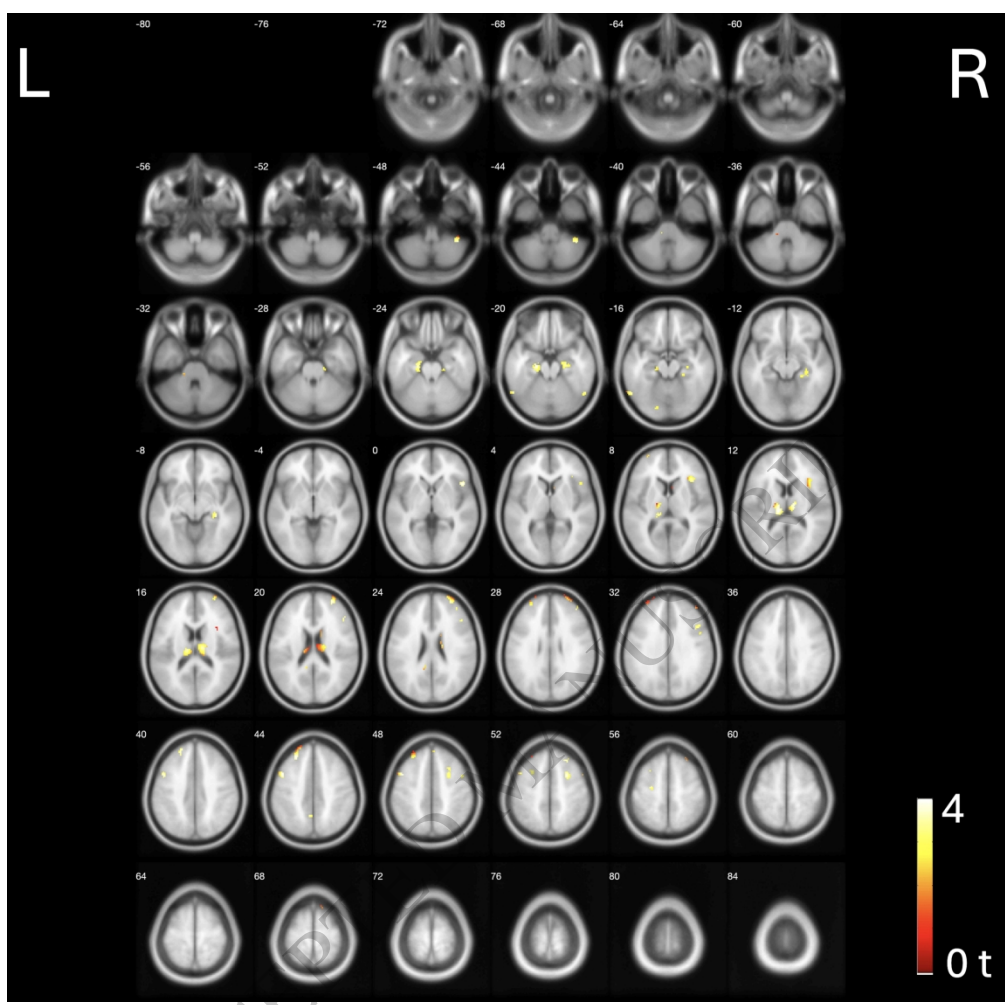


FIGURE 5: Mini-BESTest Dynamic Gait Uncorrected P=0.001
278x275mm (300 x 300 DPI)

Downloaded from <https://academic.oup.com/braincomms/advance-article/doi/10.1093/braincomms/fcae286/7741172> by Primorska University user on 30 August 2024

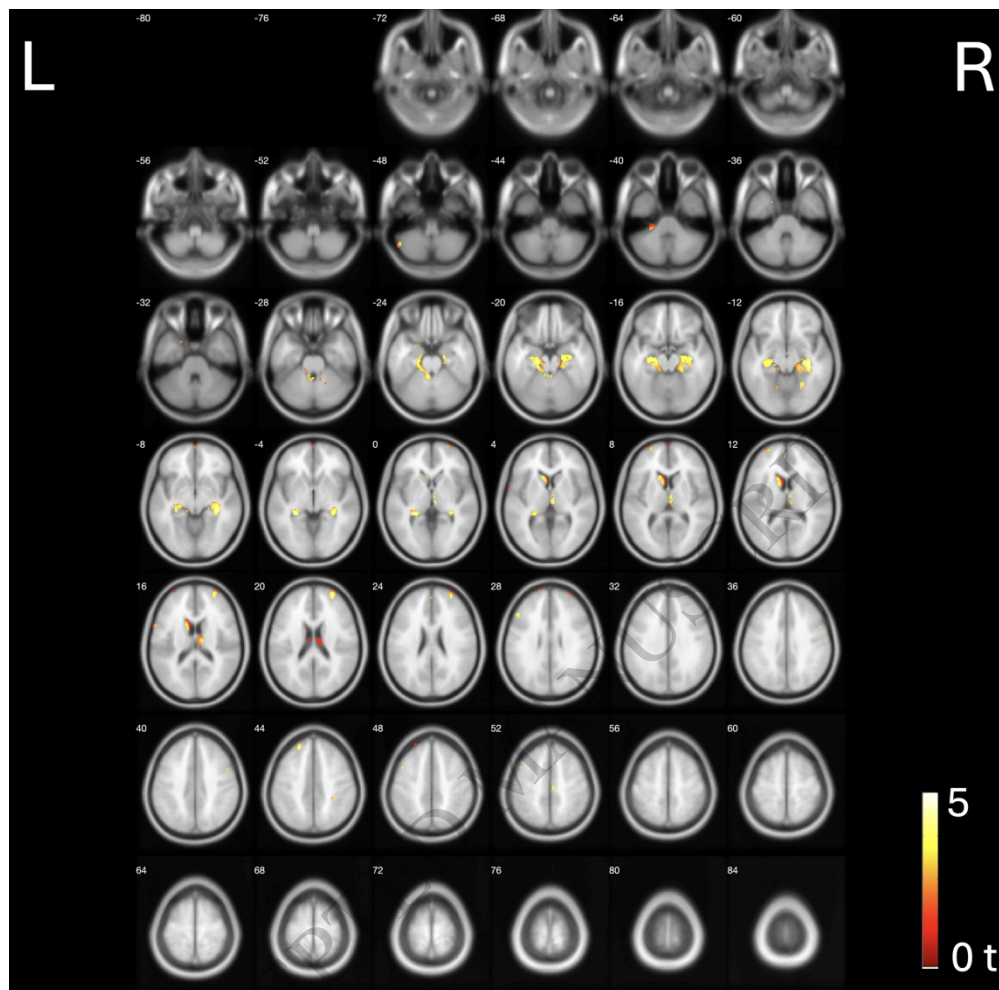


FIGURE 6: Mini-BESTest Sensory Orientation Uncorrected $P=0.001$

278x274mm (300 x 300 DPI)

ACCEPTED

1
2
3
4
5
6
7
8
9
10
11
12
13
14
15
16
17
18
19
20
21
22
23
24
25
26
27
28
29
30
31
32
33
34
35
36
37
38
39
40
41
42
43
44
45
46
47

Table 1. MiniBEST subscore partial correlation matrix table with proportion of variance captured in each subscore by the other subscores

MiniBEST Subscore	R²	$\beta_{Anticipatory}$	$\beta_{Reactive}$	$\beta_{DynamicGait}$	$\beta_{Sensory}$
Anticipatory	0.481		0.214* [0.064,0.364]	0.214* [0.049,0.378]	0.407* [0.239,0.575]
Reactive	0.303	0.287* [0.085,0.49]		0.156 [-0.037,0.35]	0.197 [-0.013,0.407]
Dynamic Gait	0.41	0.243* [0.056,0.43]	0.132 [-0.032,0.296]		0.374* [0.19,0.557]
Sensory	0.501	0.391* [0.23,0.553]	0.141 [-0.009,0.291]	0.316* [0.16,0.471]	

Standardized regression coefficients for which the difference from 0 is statistically significant (as defined by coefficient P < 0.05) are bolded and marked with an asterisk. Abbreviations: R² = coefficient of determination; β = standardized regression coefficient

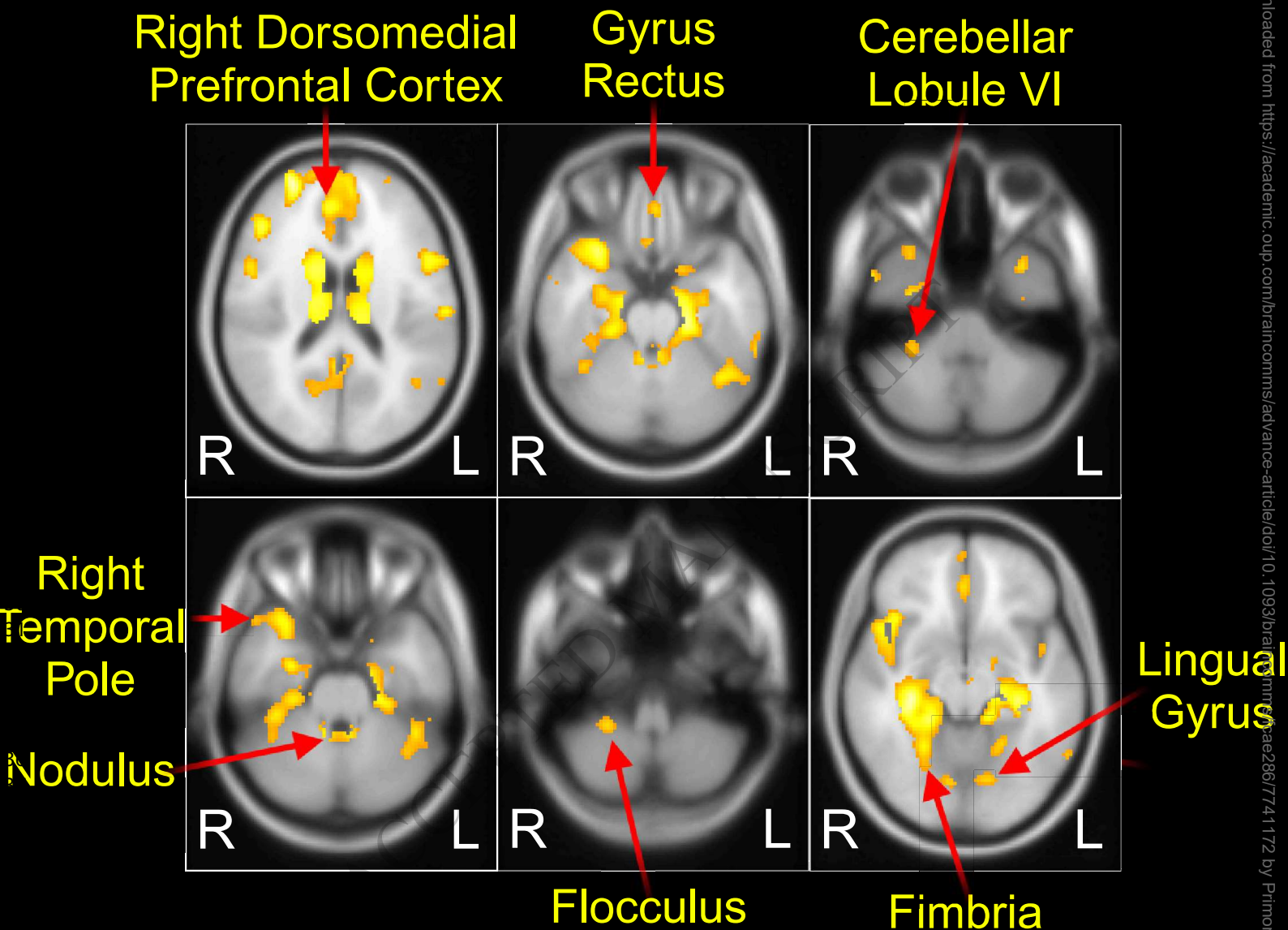
ACCEPTED MANUSCRIPT

Table 2. Summary overview of topographic system changes associating with Mini-BESTest total and sub-test scores.

FEOBV PET region	Total Mini-BESTest	APC	RPC	Dynamic gait	Sensory orientation
Gyrus rectus/orbitofrontal	B	B	B	-	-
Anterior part of the dorsomedial prefrontal cortex (upper medial BA 10 and BA 9)	R	B	R>L	-	L
Dorsolateral prefrontal cortex (BA 8 & 9)	R>L	R>L	B	R	R>L
Cingulum	all segments esp. R>L anterior and anterior mid cingulum	esp. posterior & retrosplenial segments	mainly anterior segments	equivocal posterior	-
Frontotemporal operculum	R>L	R>L	L>R	-	-
Insula	R>L	R>L	B	R	-
Mesiotemporal lobe	B	R	B	B	B (esp. hippocampi)
Fimbria	R>L	B	B	R	B
Temporal pole	R	R	R	-	-
Inferior temporal lobe	-	-	B	-	-
Mid posterior temporal lobe	L	R	L	B	-
Caudate nucleus	B	B	B	-	L
Anteroventral striatum	-	-	-	-	-
Putamen	-	-	-	-	-
LGN & MGN	B	B	B	R LGN	R > L LGN & L MGN
Thalamus proper	B	B	L pulvinar	B superior	L dorsomedial
Parietal cortex	R	-	+	-	-
Visual cortex	B	R>L	-	-	-
Lingual gyrus	R>L	R>L	-	-	R>L
Brainstem (pedunculo pontine nucleus/tectum)	-	+	-	+	+
Cerebellum flocculus	R +	-	R	-	-
Cerebellum nodulus	+	+	+	-	+
Vermis	dorsal upper vermis	dorsal upper vermis	left dorsal upper	-	-
Cerebellum hemispheres	R VI +, L crus I	R VI +	Equivocal	R VI +	L VI + L crus I
Cerebellar peduncles	B superior	B superior	B superior	-	L>R superior & L middle

^aAbbreviations: APC = anticipatory postural control; BA = Brodmann area; B= bilateral, MGN = medial geniculate nucleus; L= left, LGN = lateral geniculate nucleus; R= right, RPC= reactive postural control.

1
2
3
4



NEWLY RECOGNIZED CHOLINERGIC REGIONS ASSOCIATING WITH DYNAMIC BALANCE & GAIT IN PARKINSON'S DISEASE

Downloaded from <https://academic.oup.com/braincomms/advance-article/doi/10.1093/braincomms/286/7741172> by Primorska University user on 30 August 2024

56
57
58
59
60